

When Markets Get Confused: Misperception versus Inventory[‡]

Claes Bäckman[‡] Olga Balakina[§] Arzé Karam[¶] Anastasiia Parakhoniak^{||}

November 24, 2025

Abstract

We examine episodes in which investors mistakenly trade similarly named stocks to identify short-term, non-fundamental pricing errors. Using a long time series and a broad cross-section of U.S. equities, we systematically document the frequency, magnitude, and market response to these “confusion events”. These incidents generate pronounced abnormal returns and wider effective spreads, consistent with transient mispricing. By exploiting confusion events as exogenous, we provide new causal evidence that such dislocations primarily arise from investor misperception rather than inventory frictions. Importantly, the two channels are not mutually exclusive but represent orthogonal sources of inefficiency—belief-driven demand shocks versus dealer balance-sheet constraints. We show that in normal conditions, the misperception channel dominates, whereas under systemic stress, inventory constraints become binding. This duality bridges behavioral and structural perspectives on market inefficiency and underscores that belief errors remain a pervasive driver of transient dislocations even in deep, liquid, and technologically advanced markets.

*This research project has been supported by the British Academy/Leverhulme Grant SRG1819 \191443.

[†]We thank Konstantin Sokolov, Allen Carion, Jan Hanousek, Yeqin Zeng and seminar participants at Memphis University, SAFE and Durham University Business School for helpful comments. We gratefully acknowledge research support from the Leibniz Institute for Financial Research SAFE.

[‡]Bäckman: Leibniz Institute for Financial Research SAFE (claes.backman@gmail.com)

[§]Balakina: Leibniz Institute for Financial Research SAFE (balakina@safe-frankfurt.de)

[¶]Karam: Durham University Business School (arze.karam@durham.ac.uk)

^{||}Parakhoniak: Durham University Business School (anastasiia.parakhoniak@durham.ac.uk)

1 Introduction

Over the past two decades, financial markets have undergone a profound transformation from human-based trading to a predominantly automated structure, fundamentally reshaping how assets are priced and traded [O’hara \(2015\)](#); [Menkveld \(2016\)](#). While automation has enhanced efficiency, it has also introduced new forms of fragility: small operational or informational errors can now propagate almost instantaneously, generating distortions with real economic consequences. High-profile incidents, such as the Knight Capital collapse in 2012¹, and the May 2022 “fat-finger” event on the Stockholm OMX 30 index², illustrate how localized trading mistakes can cascade through modern market infrastructure. The recent rise of retail trading, often guided by social media narratives and heuristic attention, has further heightened concerns over mispricing. Episodes such as the 2021 meme-stock rallies highlight how sentiment shocks and collective attention can move prices even in deep and liquid markets.

In this paper, we develop a new empirical approach to identify and analyze such episodes. Specifically, we exploit ticker confusion events, i.e. instances where investors mistakenly trade a similarly named but unrelated stock—to isolate exogenous variation in order flow unrelated to fundamentals. Prior studies document that such confusion temporarily distorts trading volume and returns ([Rashes, 2001](#); [Balashov and Nikiforov, 2019](#)). We extend this idea by examining the mechanisms through which these non-fundamental shocks generate temporary price distortions. Importantly, confusion events provide a long time series for a broad cross-section of U.S. equities that we can analyze.

We distinguish between two conceptually distinct mechanisms that can both generate short-term inefficiencies. The first emphasizes inventory risk, where liquidity providers adjust quotes to manage unexpected order imbalances ([Ho and Stoll, 1981](#); [Hendershott and Menkveld, 2014](#); [Bogousslavsky and Collin-Dufresne, 2023](#)). Under this view, we should observe elevated order imbalance volatility during confusion events, consistent with market makers demanding compensation for absorbing flow ([Bogousslavsky and Collin-Dufresne, 2023](#)). The second mechanism emphasizes investor misperception and belief dispersion: confusion triggers one-sided trading driven by mistaken expectations or heterogeneous beliefs ([Asriyan, Fuchs and Green, 2019](#); [Atmaz and Basak, 2018](#)), resulting in temporary mispricing even in the absence of inventory

¹A software malfunction generated millions of erroneous orders and resulted in a \$460 million loss within 45 minutes [Kirilenko and Lo \(2013\)](#)

²It dropped 8% within minutes due to an input error.

pressures. For instance, (Asriyan et al., 2019) develop a theory of liquidity sentiments, where shifts in investor beliefs, even when not grounded in fundamentals, can lead to price and liquidity distortions. These distortions emerge from coordination failures and asymmetric beliefs, rather than dealer constraints. Similarly, Atmaz and Basak (2018) show that heterogeneous beliefs can amplify volatility and trading volume, even in the absence of inventory constraints. Under this view, confusion events trigger belief-driven trading with one-sided order flow, where liquidity deteriorates due to asymmetric or confused expectations among investors. These two mechanisms are not mutually exclusive: the former reflects constraints on liquidity supply, the latter distortions in liquidity demand. Our empirical setting allows us to isolate their relative importance.

Our results speak clearly to this debate. While confusion events produce significant abnormal returns, wider effective spreads, and volume spikes, we do not find systematic increases in order imbalance volatility. This weakens support for the inventory risk channel. Instead, several findings, including sentiment-driven price movements, weaker order flow–return linkages, and gradual reversals, are consistent with misperception and belief-based trading. In other words, confusion-induced mispricing reflects *who trades and why*, rather than market makers’ capacity to absorb flow. We define a variable measuring the speed of stock price adjustments following von Beschwitz, Keim and Massa (2020), which measures how quickly stock returns respond to information. Confusing events are generally associated with a longer time to price discovery. We also find that algorithms tend to accelerate the unwinding of misperception-driven errors, using the proxy from Hendershott, Jones and Menkveld (2011): in confusion-prone stocks with high algorithmic presence, spreads narrow more quickly and prices revert faster. This highlights a stabilizing role for algorithms in correcting non-fundamental shocks. None of these effects were found for the control group.

Our contribution is twofold. First, we introduce a novel identification strategy for studying non-fundamental price distortions based on ticker confusion. In our empirical implementation, we create *confusion-prone pairs* of two stocks whose tickers start with the same letter and are otherwise similar in nature. We select stocks traded on the NYSE and NASDAQ between 2001 and 2021, and ensure that the two companies are not in the same 4-digit SIC industry. Without loss of generality, assume that Ticker 1 is confused for Ticker 2. We use events for both tickers in a pair in the empirics. We show that Ticker 2 exhibits abnormal returns and trading volumes

across several types of events for Ticker 1, from earnings announcements to flash news. To ensure that the results are not driven by other market events, we also construct a placebo for Ticker 2 based on stock within the same industry and with the same market capitalization. We show that events for Ticker 1 do not cause any movements in trading volume or returns for Placebo Ticker 2. The findings contribute to the extensive literature on price efficiency and liquidity under informational frictions, while also shedding light on the mechanisms, i.e., inventory vs misperception, through which transitory price dislocations unfold. Our empirical strategy is designed to test these two mechanisms.

Second, we show that these price distortions are driven primarily by investor misperception rather than inventory frictions. Our findings complement prior evidence on price pressure and dealer inventory effects [Hendershott and Menkveld \(2014\)](#), but differ in showing that for small, idiosyncratic shocks, these frictions remain largely inactive. The results thus suggest that belief dispersion, rather than inventory management, drives short-term mispricing. The findings also connect our analysis to the literature on extreme price movements and the behavior of liquidity providers. [Brogaard, Carrion, Moyaert, Riordan, Shkilko and Sokolov \(2018\)](#) show that during sharp intraday returns, high-frequency traders often provide contrarian liquidity, though their capacity to absorb order imbalances is limited when multiple assets move simultaneously. Similarly, flash crashes demonstrate that inventory frictions can bind under systemic stress, leading to sharp spread widening and vanishing depth [Kirilenko, Kyle, Samadi and Tuzun \(2017\)](#). In contrast, the confusion events we study are modest in scale but far more frequent and unrelated to fundamentals, providing an ideal setting to test whether small shocks activate inventory-based liquidity constraints or instead reflect belief-driven misperception. By showing that inventory proxies remain stable while prices and spreads react strongly, our results complement evidence from extreme events and underscore the regime dependence of microstructure frictions.

Taken together, our findings extend the literature by demonstrating that even mild, non-fundamental shocks can create measurable and persistent dislocations. Whereas extreme movements reveal how dealer constraints shape liquidity under stress, our evidence shows that routine trading errors are primarily the outcome of belief dispersion and sentiment-driven misperception. These episodes illustrate that short-term deviations from fundamentals reflect noise rather than information about value. While arbitrageurs and automated traders rapidly exploit these inefficiencies to restore prices, the initial confusion still generates temporary distortions and

wider spreads until correction is complete. Confusion events therefore provide a clean empirical laboratory for understanding how markets process mistakes and for distinguishing between two key forces—misperception versus inventory frictions—in shaping short-term mispricing.

The remainder of the paper is structured as follows. Section 2 provides institutional background on U.S. equity market microstructure. Section 3 describes the data, the lexicographic identification of ticker confusion events, and the construction of key variables. Section 4 documents the empirical evidence of ticker confusion. Section 5 presents a difference-in-differences framework to estimate the causal impact of confusion events on prices and liquidity. Section 6 analyzes the competing mechanisms of market adjustment, contrasting investor misperception with inventory risk, and examines how algorithmic trading and regime dependence shape these dynamics. Section 8 concludes.

2 Institutional details related to market microstructure of US markets

Modern U.S. equity markets are fully electronic, order-driven, and highly fragmented across more than a dozen exchanges and numerous alternative trading systems. Regulation National Market System (Reg NMS) requires that all trades execute at the National Best Bid and Offer (NBBO), creating intense competition across venues. In this environment, liquidity provision is largely decentralized, with many intermediaries and algorithms simultaneously supplying quotes.

While formal market-making obligations persist, such as Designated Market Makers (DMMs) on the NYSE or Designated Liquidity Providers on NASDAQ, these commitments are relatively weak compared to historical specialist system. DMMs are required to quote a minimum proportion of the trading day, but their capital commitments are modest relative to daily turnover. As a result, no single intermediary is responsible for absorbing large order imbalances, and the system relies instead on competition among many algorithmic liquidity providers.

Algorithmic and high-frequency traders (HFTs) now account for a majority of trading volume in U.S. equities. By early 2000s, algorithmic trading accounted for less than 10% of equity shares, but it grew rapidly, capturing about 70% of the US securities by the end of 2009. Consequently, the number of quotes reported by Trades and Quotes (TAQ) has soared. To keep pace with

these developments in algorithmic trading, the Securities and Exchange Commission (SEC) has focused on enhancing market transparency and stability through advanced monitoring and diagnostic tools.³ These tools help detect and mitigate errors in real-time, ensuring a more stable and efficient market. Further, exchanges such as NASDAQ and NYSE, employ advanced diagnostic tools and machine learning to detect errors such as irregular trading patterns, network issues, or market abuse, hence ensuring smooth operations.

These electronic market makers supply liquidity by continuously arbitraging across venues, narrowing spreads, and enforcing the NBBO across fragmented markets. Prior research shows that HFTs frequently provide contrarian liquidity during stress events, helping stabilize order books (Brogaard, Hendershott and Riordan, 2014; Brogaard et al., 2018). These findings imply that temporary, non-fundamental shocks, such as ticker confusion events, are often corrected rapidly. At extreme events such as Flash Crashes, however, the previous literature has shown that liquidity provision temporarily vanishes and spreads widen dramatically (Kirilenko et al., 2017; Brogaard et al., 2018). These findings underscore that inventory risk can become highly relevant in rare, tail events. Our empirical tests provide a natural setting to observe whether such shocks impose inventory costs on liquidity providers or instead reflect mistaken demand-side trading.

Overreaction in the market refers to the excessive response of market prices to an information or misinformation. As we highlight later in the paper, it is necessary to take into account differences in price speed reaction when analyzing the effects of algorithmic trading activity on market quality around name confusion events. Algorithms are programmed to be rational and profit-maximizing. We expect non-fundamental news such as name confusion events to lead to an overreaction in the market, causing prices and trading volumes to react faster to these errors.

3 Data and Identification of Confusion

We obtain daily stock data from NASDAQ and NYSE common stocks from the Centre for Research in Security Prices (CRSP). Our sample includes the data for companies traded on NYSE and NASDAQ between January 1, 2001, and December 30, 2021. To capture the institutional response, we rely on high-frequency data from the Trade and Quote (TAQ) database, which

³See SEC Staff Report on Algorithmic Trading in U.S. Capital Markets dated August 5, 2020.

records all trades and best quotes across U.S. exchanges. We compute effective spreads, depth at the best bid and ask, and order imbalances as standard measures of liquidity provision and potential inventory stress. We use the National Best Bid and Offer (NBBO) to compute the ex ante quoted half-spread. We mainly focus on the widely-used effective spread measure. Order imbalance volatility serves as a proxy for the intensity of inventory pressure (Bogousslavsky and Collin-Dufresne, 2023), while the correlation between order flow and returns indicates whether trades convey information or instead reflect noise. These measures allow us to test whether confusion-driven dislocations originate from liquidity providers' risk-bearing constraints or from the mistaken trading behavior of investors. Finally, we use the Ravenpack database to collect news and events.

We start with a sample of all US listed common stocks that can be matched in both TAQ and CRSP databases. To be included in our sample, the stock needs to have a price greater than \$5 and lower than \$1,000, and a market capitalisation greater than \$100 million. We only consider trades and quotes over the regular trading hours, i.e. 9:30 am to 4:00 pm. We match quotes to trades using the tick rule algorithm and apply the correction and filters for TAQ data proposed by Holden and Jacobsen (2014).

3.1 Identifying confusion-prone tickers and control groups

Our main analysis is based on co-movements between stocks with similar tickers. We now describe how we identify those events in the data. We first create a group of ticker pairs, which we will refer to as *confusion-prone pairs*. To create our confusion-prone group, we take tickers of all companies that were traded on the NYSE and NASDAQ between January 1, 2001, and December 30, 2021. We then identify pairs that satisfy two conditions: a) Ticker 1 and Ticker 2 start from the same letter, and b) the Levenshtein distance between Ticker 1 and Ticker 2 is equal to one. Levenshtein distance is a metric used to measure the difference between two sequences of strings. It calculates the total minimum number of single-character edits (such as deletion, insertion, and substitutions) required to change one string to another (Levenshtein, 1966). For example, ABCD and ACBD differ only due to the location of the letter B, and so have a Levenshtein distance of one. Moving B in the second string back one position makes the two strings identical.

We apply an additional data filter to avoid ambiguity in identifying ticker confusion. For

example, there are groups of tickers where the Levenshtein distance between all tickers is 1 (e.g. *ABCD*, *ACBD*, *ABBD*), and there are clusters of tickers where each ticker in a cluster has a distance of one from at least one another ticker in the same cluster, but some pairs of tickers have the distance larger than 1 between them (e.g. *ABCD*, *ACBD*, *ACBQ*). We therefore focus exclusively on pairs of tickers that are uniquely identified based on their similarity. In the next step, we control for the industry codes of tickers in each pair. If Ticker 1 and Ticker 2 belong to the same industry, then informative events related to Ticker 1 may also be relevant for Ticker 2 due to competitive dynamics, common industry shocks, or spillover effects. To ensure that an informative event for Ticker 1 is not informative for Ticker 2, we use 4-digit industry codes from CRSP database to exclude all pairs that belong to the same industry.

This approach is designed to capture the types of mistakes that are most likely to generate ticker confusion in practice. Traders may accidentally press a neighboring key on the keyboard, omit or add a single letter, or transpose two adjacent letters when entering an order. All of these errors produce a mistyped ticker that differs only slightly from the intended one. By restricting attention to pairs with a Levenshtein distance of one and the same initial letter, we isolate cases where the erroneous ticker still looks very similar to the correct one—similar enough that a trader, an algorithm, or even an automated news-parsing system could plausibly mistake one for the other.⁴ This ensures that our “confusion-prone pairs” reflect realistic, minimal-error scenarios rather than broader similarities that would be unlikely to cause genuine confusion.

3.2 Identifying events

We use the Raven Pack database to identify dates and timestamps for events. The database contains various types of news, including but not limited to press releases, news flashes, and full articles. Our primary focus is on press releases, which are often followed by other types of news on the same day. News flashes typically appear within a few minutes. There may be multiple press releases issued on the same day, sometimes within seconds or minutes of each other. In many cases, if a second press release is issued more than 30 minutes after the first, it is considered a follow-up to the initial report. Consequently, we use the timestamp of the first

⁴Why we think that these mistakes look more human-driven, we can still think about the scenarios where news-scraping algorithms, sentiment-analysis tools, and automated data-ingestion pipelines often rely on text sources—such as press releases, social media, or unstructured documents—where tickers may be misspelled or ambiguously formatted. In such cases, an algorithm that uses approximate string matching or imperfect parsing rules could easily misidentify a ticker that differs by only one character or involves a simple transposition.

press release issued during the day as the event timestamp. After that, we exclude from our samples all events for Ticker 1 if Ticker 2 was not traded on the event day. We also exclude all events where there was an informative event for Ticker 2 either on the same day, day before or day after the event for Ticker 1. Finally, we exclude from our confusion-prone sample all events where Ticker 2 was traded less than 30 minutes after the event announcement on the event day. The final sample includes 998 events for the confusion-prone group.⁵ Most of the events in our final sample occur during the post-decimalization period, when the NYSE market structure transitioned to automation. Additionally, a small number of events are from the 2001-2004 period and include stocks that were traded on NASDAQ. The distribution of identified events in our samples across different years is illustrated in Figure 2.

3.3 Control samples

We also create control samples. For each control sample, we take the same events as in the confusion-prone sample, but rematch Ticker 1 with a new ticker, denoted Ticker 2', for event i based on the following criteria: (a) Ticker 2', starts with a different letter than Ticker 1, (b) the Levenshtein distance between Ticker 1 and Ticker 2', is greater than one, (c) Ticker 2' is in the same quintile of market capitalization as Ticker 2 on the day preceding the event, and (d) Ticker 2' has the same industry code as Ticker 2.

We create two control samples that satisfy conditions (a) - (c), and one control sample that satisfies conditions (a)-(d). Condition (d) is quite restrictive, and we cannot always find a match that satisfies all four conditions. Therefore, the size of the control group, where we also check the industry code, is reduced to 717 events. Nevertheless, all our primary results are reported based on the control sample that includes the industry code check.

3.4 Variables

Abnormal return. We download trading data for each event in the sample on the event date, the trading day before, and the trading day after the event from the TAQ database. This data is then aggregated into 1-minute bins. We use this data to compute abnormal returns $AR_{i,t}$

⁵Notice that if tickers $ABCD$ and $ABCE$ are identified as a pair satisfying the conditions described above, we include in the sample all events where $ABCD$ is Ticker 1 and $ABCE$ is the potentially confusion-prone Ticker 2. Similarly, we also include all events where $ABCE$ is Ticker 1 and $ABCD$ serves as Ticker 2, which could potentially be affected by name confusion. In the analysis of Section 6.3, additional events are excluded from the confusion-prone and control groups where there is missing data for control variables. This will be discussed later on.

as

$$AR_{i,t} = R_{i,t} - \frac{1}{T_0} \sum_{\tau=1}^{T_0} R_{i,\tau}, \quad (1)$$

where $R_{i,t}$ is return of stock i , t minutes after the event, and $\frac{1}{T_0} \sum_{\tau=1}^{T_0} R_{i,\tau}$ is the average return in the estimation window. T_0 - length of estimation window. We also compute cumulative abnormal returns: $CAR_i = \sum_{t=1}^T AR_{i,t}$. For our analysis, we select an estimation window of 1 hour prior to the event and set the length of the event window to 1 hour after the event.

Algorithmic trading activity. Following [Hendershott et al. \(2011\)](#), we use a proxy of algorithmic trading (AT) defined as the negative of trading volume (in hundred of dollars) per minute divided by the number of electronic messages. An increase in this measure reflects an increase in AT activity.⁶

Effective spread. We use the effective spread as our main measure of liquidity. The percent effective spread of trade t on stock i is widely used in the literature and defined as: $EffectiveSpread_{i,t} = 2|\ln P_{i,t} - \ln M_{i,t}|$; where $P_{i,t}$ is the trade price and $M_{i,t}$ denotes the mid-point of the best quote available immediately preceding the trade. To measure non-fundamental trading activity around named-inducing events, we compute dollar trading volume as a measure of volume, since it is the volume associated with the effective spread. We also compute the quoted spread as the difference between the best ask and the bid, and the quoted depth as an average time-weighted share depth at the best bid and the best ask in one-minute interval. We also compute the realized volatility as our measure of volatility consistent with [Andersen, Bollerslev, Diebold and Ebens \(2001\)](#).

Speed of stock price response. We rely on the approach in [von Beschwitz et al. \(2020\)](#) to define a Speed of stock price response (SSPR) variable. For the purposes of our analysis, for each event i , we calculate the $SSPR_i$ variable at time t as the ratio of the absolute return in 1a -minute interval from t to $t + 1$ for Ticker 2 divided by the sum of absolute returns from t to $t + 1$ and from $t + 1$ to $t + 60$.

$$SSPR_{i,t} = \frac{Abs(Return_i(t, t + 1))}{Abs(Return_i(t, t + 1)) + Abs(Return_i(t + 1, 60))},$$

where $t \in [0, 60]$ - time after the event, $Abs(Return_i(t, t + 1))$ is an absolute value of the

⁶The measure is always below zero. Thus, it is increasing if the value goes from a smaller negative number to a larger negative number. In absolute terms, the value decreases with an increase in algorithmic activity.

return for every minute after the event, $Abs(TotalRetur_i(t + 1, 60))$ is the absolute value of the cumulative abnormal return after the minute $(t + 1)$ till the end of the two hour period.

$SSPR_{i,t}$ measures how much return every minute explains of the remaining total return, and SSPR measures the speed with which return’s explanatory power changes over time. The speed of stock adjustment decreases with time if markets are efficient. Higher price adjustment indicates faster discovery of the true price of the asset and signifies more efficiency on the market.

If we expect that the confusion leads to higher abnormal returns, and then we observe the correction later on, then we should expect that this variable should decrease over time in the interval from $t \in [0, 60]$. Therefore, we construct a variable $\Delta SSPR_{i,t}$, which measure the change in the speed of price reaction.

$$\Delta SSPR_{i,t} = SSPR_{i,t} - SSPR_{i,t-1} \quad (2)$$

3.5 Summary Statistics

Table 1 reports descriptive statistics for Confusion-prone tickers and the control groups with dissimilar tickers. To better understand the assets in confusion-prone and control groups, Table 1 examines returns, price, volume, algorithmic activity and liquidity metrics for the full sample in Column (1), for the sample of confusion-prone stocks in Column (2), and for our primary control group where we control for the industry NAICS code in Column (3). The t-statistics reported in Column (4) capture whether there is a significant difference in some parameters between confusion-prone tickers in Column (2) and control units in Column (3). We note that volatility and turnover are higher for confusion-prone stocks as opposed to the control group, which is logical if our confusion-prone group includes confusion among investors. Additionally, we observe that algorithmic trading activity prior to the event (ALGO Trading, before) is higher for confusion-prone stocks, with the difference being statistically significant at the 5% level. However, this difference disappears once we look only at the events where associated algorithmic trading activity is above median. This observation will be important for the discussion of the results in Section 6.3.

4 Evidence of Confusion

This section documents how confusion events affect prices, volume and liquidity, setting the stage for testing whether distortions arise from inventory friction or investor misperception.

4.1 Abnormal reactions and market overreaction

We first establish that confusion events lead to significant market overreactions in confusion-prone pairs. These errors can cause sudden and dramatic price movements, as the market reacts to the unexpected volume. For this, we measure the abnormal cumulative returns and trading volume of the confusion-prone group to those of a control group. By design, the only distinction between these groups is the likelihood of confusion with stocks that have similar tickers to the event tickers. We then conduct multiple tests to determine whether there are significant differences in stock reaction behavior between the confusion-prone and control groups, which could indicate the presence of confusion in the confusion-prone group.

Confusion-prone stocks exhibit clear market overreactions following events for similarly named tickers. In Figure 3, we plot the average CARs across different time bins for both the control and confusion prone tickers to analyze their behavior before and after an event. The plot reveals that the average CARs for the confusion prone tickers are considerably larger in magnitude after the event. Cumulative abnormal returns in the 60-minute window after the event are significantly larger and more dispersed than those of matched controls. In general, the magnitude of the CAR is similar to the results reported by [Balashov and Nikiforov \(2019\)](#) for various types of events. Table 2 provides additional support, showing the means and deciles of CAR distributions for both groups. The table confirms that confusion-prone stocks exhibit more frequent extreme positive and negative CARs compared to the control group. While CARs for control stocks cluster around zero, confusion-prone stocks display wide tails, with frequent large positive and negative returns. This asymmetric and volatile reaction pattern suggests a non-fundamental shock, either liquidity providers reacting to sudden one-sided order flow or investors mistakenly trading on confused beliefs. We later test these different hypotheses.

4.2 Spread and algorithmic activity

Figure 4 plots the evolution of effective spreads in a ± 60 -minute window around confusion events and their matched controls. In the pre-event period, spreads for both groups overlap closely,

indicating comparable baseline liquidity and no anticipation of the forthcoming shock. At $t = 0$, spreads for confusion events widen sharply—peaking within roughly five minutes—before gradually reverting toward control levels. This transient widening reflects a short-lived increase in transaction costs as dealers absorb the sudden imbalance in order flow. The absence of any pre-event divergence rules out inventory pre-positioning or anticipatory volatility, reinforcing the interpretation that confusion shocks originate from unexpected, belief-driven trading rather than from deteriorating liquidity conditions.

Figure 5 reports the mean Algorithmic Activity Index (AAI) within a ± 60 -minute window for confusion prone tickers and matched control events. The AAI measures the number of order-book messages—NBBO updates and trades—per \$100 of traded value, providing a normalized gauge of automated execution intensity. The figure shows a pronounced surge in algorithmic activity during the five minutes immediately preceding confusion events, while controls remain nearly flat. This timing pattern suggests that automated trading systems increase message traffic immediately before the onset of mispricing, consistent with high-frequency slicing or routing errors rather than strategic information trading. Because spreads and volatility remain stable before the shock, the rise in AAI represents the mechanical propagation of mistaken orders under otherwise normal market conditions. Together, Figures 4 and 5 show that confusion shocks emerge endogenously through automated execution in a liquid environment and that price distortions arise not from ex-ante stress but from algorithmic amplification of misperceived demand.

4.3 Robustness and additional tests

We now discuss several other tests that strengthen the conclusion that confusion events cause abnormal price movements. A key empirical concern with ticker confusion is separating genuine mistakes from other correlated shocks. Similar-looking tickers may belong to firms that share unobserved traits, making them prone to co-movement for reasons unrelated to confusion. Note that our control group includes firms in the same industry with similar market capitalization. If our confusion-prone pairs were simply capturing unobserved traits, such as exposure to a certain industry or a size effect, we would expect to see some evidence of abnormal returns also here. The lack of response in control firms to events is thus reassuring. Recall also that the summary statistics provided little evidence of difference in observable characteristics. Finally, it is also reassuring that our results are consistent with the previous literature (Rashes, 2001;

Balashov and Nikiforov, 2019). For example, Balashov and Nikiforov (2019) show evidence that when ticker names change, the confusion stops. This is again evidence for a genuine effect of ticker confusion on abnormal returns.

Nonetheless, there may be unobserved factors that cause abnormal returns. We therefore conduct two more tests to provide more evidence in line with ticker confusion. Specifically, we test whether sentiments related to events predict abnormal returns, and whether there is correlation in price direction. We now describe these tests.

Sentiment alignment and directional trading

If misperception drives confusion events, the price of the confused stocks should move in the same direction as the sentiment of the news. As the next step, we investigate whether the abnormal price response of Ticker 2 of confusion-prone stocks following an event for Ticker 1 can be explained by the sentiment associated with the event for Ticker 1. von Beschwitz et al. (2020) show that machine learning-based news analytics used by investors to interpret financial news affect stock prices and trading volume. We use the Composite Sentiment Score from Ravenpack to investigate whether market overreaction for confusion-prone stocks is in the direction of the sentiment. This score ranges from -1 (extremely negative) to +1 (extremely positive) and combines various sentiment measures, including the price reaction to the news. In our context, we expect CARs of confusion-prone stocks to be positively correlated with the Composite Sentiment Score. Specifically, if the abnormal reaction is driven by stock confusion, we would expect events with higher positive sentiment scores to yield higher positive abnormal returns. Conversely, events with neutral sentiment may attract less investor attention and, therefore, result in little or no reaction. To test this hypothesis, we estimate the following equation:

$$CAR_{i,t}^2 = \alpha + \beta CSS_{i,t}^1 + \gamma X_{i,t} + \epsilon_{i,t},$$

where $CAR_{i,t}^2$ is the absolute cumulative abnormal return for Ticker 2 (the confused stock), $CSS_{i,t}^1$ is the Composite Sentiment Score for Ticker 1 (the event stock), and $X_{i,t}$ are controls, which include log market capitalization, log turnover and a dummy for above median algo activity. The results in Table 3 show that for confusion-prone stocks in the first three columns, CARs are positively correlated with the Composite Sentiment Score. Using the coefficient in the first column, we find that a one standard deviation increase in CSS predicts a 0.06

standard deviation increase in the cumulative abnormal return. The CARs for the control group in columns 4-6, however, do not exhibit this correlation. These findings lean toward the belief-driven misperception mechanism, where investors react to sentiment cues rather than fundamentals.

4.4 Correlation in returns

Next, we evaluate whether short-term price movements (returns) for confusion-prone and control stocks are correlated with short-term returns for Ticker 1. In the absence of common market trends, we would not expect a significant correlation between the returns of stocks in the control group. In contrast, if ticker confusion is present, we expect a positive correlation in the magnitude of price changes for the confusion-prone group.

To assess the correlation in price movements across control and confusion-prone groups, we estimate the following regression model:

$$R_{i,t}^{tick2} = \alpha_i + \beta_1 R_{i,t}^{tick1} + \beta_2 R_{i,t-1}^{tick1} + \beta_3 R_{i,t-1}^{tick2} + \epsilon_{i,t}, \quad (3)$$

where $R_{i,t}^{tick1}$ is the return for Ticker 1 at time t , the primary variable of interest, capturing whether the return on Ticker 1 is associated with a contemporaneous return on Ticker 2. We also include $R_{i,t-1}^{tick1}$ and $R_{i,t-1}^{tick2}$ to examine pre-trends and potential autocorrelation in returns.

Table 4 reports the results. We find a significant correlation in returns between Ticker 1 and Ticker 2 for the confusion-prone group. The positive coefficient β_1 for the confusion-prone group indicates that returns on Ticker 2 move in the same direction with returns on Ticker 1. In contrast, no such correlation is observed in the control group. This pattern is consistent with investors trading the wrong asset based on the perceived signal from the correct ticker, reflecting demand-side misperception.

Taken together, the evidence from returns, sentiment, and price correlations supports the view that demand-side misperception drives mispricing, paving the way for the next section's formal tests of whether liquidity providers' inventory constraints play a role.

5 The Effect of Ticker Confusion on Liquidity and Inventory

This section quantifies how ticker confusion affects market liquidity and dealer inventory risk using a stacked event–time difference-in-differences (DiD) design. The stacked framework aligns all events in relative time, allowing dynamic treatment effects to be estimated while absorbing overlapping windows and heterogeneous announcement timing.

5.1 Market Reaction and Spread Dynamics

We estimate the following event–time specification:

$$\log(\text{EffectiveSpread}_{i,e,k}) = \sum_{b \in \mathcal{B}} \theta_b (\text{ConfusionProne}_i \times \mathbf{1}\{k \in b\}) + \alpha_i + \psi_e + \mathbf{X}'_{i,e,k} \gamma + \varepsilon_{i,e,k}, \quad (4)$$

where i indexes tickers, e indexes events, and k denotes relative minutes within the event window. \mathcal{B} partitions relative time into bins $[-60, -31]$, $[-30, -11]$, $[0, 10]$, $[11, 30]$, and $[31, 60]$, with $[-30, -11]$ as the baseline and $[-10, -1]$ omitted to avoid information leakage. Ticker and event fixed effects (α_i, ψ_e) capture persistent heterogeneity, and $\mathbf{X}_{i,e,k}$ includes controls for log turnover and log return volatility. Standard errors are two-way clustered by (event \times pair) and by relative-minute following [Thompson \(2011\)](#).

Identification and Interpretation. The identification follows a standard difference-in-differences logic. Each coefficient θ_b measures the average change in liquidity for confusion-prone (treated) tickers relative to their matched controls, net of any baseline difference prior to the event. Formally, it captures

$$\theta_b = (E[Y_{\text{ConfusionProne}, k \in b} - Y_{\text{ConfusionProne}, \text{pre}}]) - (E[Y_{\text{control}, k \in b} - Y_{\text{control}, \text{pre}}]),$$

so that the estimated effect reflects the differential deviation of confusion prone tickers versus control tickers from their respective pre-event levels. Ticker fixed effects (α_i) remove any time-invariant cross-sectional differences between confusion prone tickers and control units, while event fixed effects (ψ_e) absorb shocks common to all tickers within a given announcement window. Thus, identification relies on within-ticker variation around event times and the cross-sectional contrast between confusion-prone and non-confused tickers. The statistically

insignificant pre-event coefficients reported below support the required parallel-trends assumption.

Results. Table 5 show that confusion events cause a sharp but short-lived widening in effective spreads. Pre-event coefficients are indistinguishable from zero, satisfying the parallel-trends assumption. At the event minute $k = 0$, spreads rise by roughly 11% about 4 bps at the median spread of 37 bps—and peak five minutes later near +49% (≈ 18 bps). Averaged over the first ten minutes, the effect remains about +12 % (+4.5 bps) and dissipates within 20–30 minutes. The magnitude nearly triples for high-confusion events, confirming that the liquidity shock scales with informational noise. These dynamics imply a fast but transitory contraction in liquidity consistent with belief dispersion rather than balance-sheet stress.

Table 7 show that trading volume simultaneously drops by about 13 % in the first ten minutes and remains subdued for another 20 minutes before normalizing. This temporary decline indicates that market participants pause execution amid elevated uncertainty rather than face capital constraints. Quoted depth, reported in Table 8, falls by roughly 6 % immediately after the event and fully recovers within 20–30 minutes. Depth replenishment occurs slightly earlier than spread normalization, consistent with market-makers defensively pulling quotes and then re-entering once noise subsides.

Overall, the event-time evidence depicts a coherent intraday liquidity cycle: spreads widen, depth thins, and volume falls—all sharply but briefly. The absence of persistent effects suggests that confusion events trigger short-term informational frictions rather than structural funding stress. Liquidity providers widen quotes to price transient uncertainty, not to manage binding inventory constraints.

5.2 Inventory Risk Channel

To test whether spread widening reflects dealer inventory pressure, we examine the volatility of signed order imbalance (OI) following [Bogousslavsky and Collin-Dufresne \(2023\)](#). If confusion forced dealers to absorb unbalanced flow, the short-run volatility of OI should rise alongside spreads.

Trades are signed using the quote-based algorithm of [Holden and Jacobsen \(2014\)](#) and [Chakrabarty,](#)

Li, Nguyen and Van Ness (2007). For each five-minute interval t ,

$$OI_{i,t} = \frac{BuyCount_{i,t} - SellCount_{i,t}}{BuyCount_{i,t} + SellCount_{i,t}} \quad (5)$$

and short-horizon order-imbalance volatility is

$$VolOI_{i,e,k} = \sqrt{\frac{1}{4} \sum_{t=1}^5 (OI_{i,t} - \overline{OI}_i)^2}. \quad (6)$$

We estimate an analogous stacked specification:

$$\log(VolOI_{i,e,k}) = \sum_{b \in \mathcal{B}} \theta_b^{(OI)} (ConfusionProne_i \times 1\{k \in b\}) + \alpha_i + \psi_e + \mathbf{X}'_{i,e,k} \gamma + \mathbf{D}'_{i,e,k} \mu + \varepsilon_{i,e,k},$$

where $(\mathbf{D}_{i,e,k})$ adds bid- and ask-depth controls; bins and clustering match Equation (4).

Results. Table 6 show that OI volatility remains essentially flat around confusion events. All post-event coefficients are small (0.00–0.01) and statistically indistinguishable from zero, with joint p -values above 0.6. These null effects stand in stark contrast to the pronounced but short-lived spread widening. Adding controls for turnover, volatility, and depth yields qualitatively identical results, indicating that liquidity providers do not experience heightened inventory stress.

Interpretation. The combined evidence indicates that ticker confusion primarily generates belief-driven mispricing and transient noise trading rather than structural liquidity shocks. Liquidity providers momentarily widen spreads and withdraw depth to price informational uncertainty, but inventories remain balanced and depth quickly replenishes. Volume normalization within 30 minutes confirms the absence of sustained trading pressure. Thus, confusion events disrupt the information aggregation process rather than dealers' balance sheets, producing short-lived liquidity frictions rooted in sentiment and attention rather than funding constraints.

6 Competing Mechanisms and Algorithmic Correction

Building on the evidence that belief dispersion, rather than inventory frictions, drives confusion-induced distortions, we now explore how markets correct these errors. We examine the roles of algorithmic trading, sentiment spillovers, and liquidity conditions in shaping the speed and

magnitude of price corrections. We also test whether these dynamics vary across market regimes, i.e. normal versus stress conditions, where inventory constraints may re-emerge.

6.1 Speed of price adjustments

We first analyze how quickly prices adjust following confusion events and whether algorithmic trading accelerates the correction of misperception-driven errors. Specifically, we test whether algorithmic activity shortens the duration of mispricing using the following specification:

$$\Delta SSPR_{i,t} = \alpha + \beta_1 \times ConfusionEvent_i + \beta_2 \times Algo_{i,t} + \beta_3 \times ConfusionEvent_i \times Algo_{i,t} + \epsilon_{i,t}.$$

where *ConfusionEvent* is a dummy equal to one for the pair-event with confused tickers, and zero for the control group pair-events, *Algo_{i,t}* is the proxy for algorithmic trading associated with the Ticker 2 in the pair, and $\epsilon_{i,t}$ is an error term. We are interested in the coefficient β_3 . If β_3 is negative, i.e., the amount of subsequent cumulative return explained by 1-minute return at time t is dropping faster in the presence of higher algorithmic activity. A positive β_3 signifies that algorithmic trading does not improve the price discovery around confusion events. Note that the data is defined post-event, and so there is no *After* variable in this setting. Intuitively, β_1 tests whether price discovery takes longer in confusion events, and β_3 tests how algorithms change price discovery during confusion events.

Table 9 reports the estimation results. First, we see that on average in the event of confusion, price discovery takes longer: the estimated coefficient β_1 is positive and significant. The coefficient on $ConfusionEvent_i \times Algo_{i,t}$ shows higher algorithmic activity offsets this delay as shown in the negative and significant β_3 . The separate regressions for two event types, Confusion (2) and Control (3), show that the algorithmic trading effect shows up only for the confusion events. This pattern supports the view that algorithms act as corrective forces rather than amplifying the errors.

Figure 6 compares market reactions between confusion-prone and control stocks around event time. Across all dimensions (return volatility, absolute cumulative abnormal returns (—CAR—), and the flow–return sensitivity β), we observe pronounced differences. Confusion stocks exhibit a sharp but short-lived surge in return volatility and —CAR— immediately following the event, whereas control stocks remain stable. These volatility bursts coincide with weakened flow–return

relationships, consistent with trading driven by belief dispersion rather than information or inventory needs. Within an hour, both volatility and —CAR— converge back to pre-event levels, indicating rapid correction of mispricing. Together, these results confirm that ticker confusion induces transient, non-fundamental price pressure that algorithms and informed traders quickly arbitrage away, restoring market efficiency within the same trading hour. This further supports the misperception hypothesis: confused stocks co-move with the sentiment of unrelated news, order flow becomes less informative, and returns partially reverse over time.

6.2 Confusion vs. Control: Liquidity Responses

We now examine how market liquidity and trading activity respond during confusion events relative to matched controls. We analyze three complementary dimensions: (i) *trading costs and order-flow risk*, (ii) *book resiliency and trading intensity*, and (iii) *price impact per unit of order flow*. Together these diagnostics reveal whether confusion events create transient belief-driven noise or deeper liquidity-provider frictions.

Trading Costs and Order-Flow Risk Figure 7 contrasts transaction costs and order-imbalance volatility between confusion and control stocks. Panel (A) shows that effective spreads widen modestly around the announcement minute for confusion stocks, indicating a short-lived increase in trading costs. Panel (B) reports the standard deviation of order imbalance in 15-minute intervals. Imbalance volatility remains broadly stable, suggesting that liquidity providers do not face binding inventory constraints. The absence of a volatility spike supports a *belief-dispersion* rather than an *inventory-friction* interpretation.

Book Resiliency and Trading Intensity Next, Figure 8 examines how posted liquidity and trading intensity evolve. Panel (A) shows a temporary dip in total depth (sum of bid and ask) that quickly refills within minutes. Panel (B) shows a sharp but short-lived surge in trading volume. Both indicators normalize within an hour, demonstrating that order-book resiliency remains intact and that the market rapidly absorbs non-fundamental order flow.

Finally, Figure 8 also links order imbalance to price impact. Panel (C) plots log-demeaned absolute order imbalance, $\log |OI| - \overline{\log |OI|}_{[-60,-5]}$, which rises briefly at the event and reverts quickly. Panel (D) shows Kyle’s $\lambda = |Return|/(|OI| + \varepsilon)$, normalized to its pre-event mean. The spike and rapid reversion of λ indicate that confusion-driven mispricing is swiftly corrected,

consistent with high-frequency arbitrage restoring informational efficiency rather than with dealers rebalancing inventories.

Interpretation. Across trading costs, order-book depth, and price-impact measures, confusion events cause short-lived dislocations that fade within 30–60 minutes, while control stocks remain stable. These findings reinforce the view that ticker confusion reflects *temporary misperception* rather than persistent *inventory frictions*. Collectively, the results provide or not evidence that confusion-induced trading represents belief contagion rather than liquidity-provider stress.

6.3 Algorithms and the Magnitude of Confusion

This section investigates how the dynamic impact of ticker confusion on liquidity varies with algorithmic trading intensity. We extend the stacked event–time difference-in-differences (DiD) design from Section 5 to compare the response of market quality variables for stocks with high versus low algorithmic participation prior to the event. The design isolates how algorithms modulate the propagation and resolution of belief-driven shocks in real time.

Specification. For each event e , we estimate a stacked DiD model of the form:

$$\log(s_{i,e,k}) = \sum_{b \in \mathcal{B}} \theta_b^{(AT)} (\text{HighAT}_i \times \text{ConfusionProne}_i \times 1\{k \in b\}) + \alpha_i + \psi_e + \mathbf{X}'_{i,e,k} \gamma + \varepsilon_{i,e,k}, \quad (7)$$

where $s_{i,e,k}$ is the effective spread (in bps) for stock i in relative minute k around event e . \mathcal{B} defines event-time bins $[-60, -31]$, $[-30, -11]$, $[0, 5]$, $[6, 20]$, and $[21, 60]$, with $[-30, -11]$ serving as the reference period and $[-10, -2]$ omitted to avoid leakage. The coefficient $\theta_b^{(AT)}$ captures the differential dynamic response of spreads for high–algorithmic trading (High-AT) stocks relative to low-AT stocks within the confusion-prone group. Ticker and event fixed effects (α_i , ψ_e) absorb persistent heterogeneity, and controls $\mathbf{X}_{i,e,k}$ include log turnover and return volatility. Standard errors are clustered two ways—by (event \times pair) and by relative minute.

Results. Figure 9 plots the estimated $\theta_b^{(AT)}$ coefficients. The spread dynamics differ sharply across algorithmic intensity regimes. For high-AT stocks, spreads rise modestly following con-

fusion events and revert to baseline within ten minutes, whereas for low-AT stocks, spreads widen sharply and remain elevated through the next 20 minutes. Joint pre-trend tests confirm that the identifying assumption holds for the high-AT subsample ($\chi^2(5) = -1.94$, $p = 1.000$; average pre-trend $\chi^2(1) = 0.081$, $p = 0.776$) but fails for the low-AT group ($\chi^2(5) = 1209.06$, $p < 0.001$), indicating that the high-AT specification provides credible causal inference.

Window-average results reported in Table 10 quantify these differences. In the first five minutes after a confusion event, effective spreads are on average 42% (≈ 16 bps) higher in low-AT than in high-AT stocks. By minutes 6–20, the difference dissipates and becomes statistically insignificant (-11% , 95% CI includes zero). The short-lived differential suggests that algorithmic participation dampens the amplitude and duration of belief-driven liquidity shocks, consistent with a stabilizing role in market microstructure.

Interpretation. The combined evidence indicates that algorithmic participation mitigates confusion-induced mispricing by accelerating information diffusion and restoring price efficiency. In markets with active algorithmic trading, belief-driven dislocations unwind rapidly, consistent with high-frequency traders supplying liquidity and arbitraging transitory mispricing. Conversely, when algorithmic participation is low, transient confusion translates into wider and more persistent spreads, reflecting slower market learning and thinner liquidity. These dynamics highlight the conditional stabilizing role of algorithms: they do not eliminate confusion but compress its impact in time and magnitude.

6.4 Regime Contrast: Confusion versus Extreme Events

We next examine whether the observed mechanisms are regime-dependent by contrasting *confusion events* with *extreme events*, defined as the top 1% of intraday return realizations. During extreme events, order imbalance volatility and spreads surge, while market depth declines sharply, consistent with dealers facing binding inventory constraints. In contrast, during confusion events, these variables remain largely flat. This contrast illustrates that under normal conditions, belief dispersion dominates, whereas under market stress, inventory frictions become binding.

Figure 10 highlights this regime dependence in market adjustment. During extreme events, order-imbalance volatility rises steeply, effective spreads widen, and market depth collapses—signatures of transient liquidity shortages. This pattern aligns with the inventory-friction mechanism of

Brunnermeier and Pedersen (2009), where limited funding and risk capacity lead market makers to scale back inventory provision. In contrast, during confusion events, order-imbalance volatility and liquidity measures remain nearly flat, showing no evidence of liquidity withdrawal or elevated inventory pressure. Ticker confusion thus represents a primarily *belief-driven distortion*: transient misperception, rather than risk-bearing constraints, drives mispricing.

While we find little evidence that inventory constraints amplify confusion-induced shocks on average, the two mechanisms are not mutually exclusive. The belief-dispersion channel and the inventory-risk channel represent orthogonal sources of temporary inefficiency: one arises from *who trades and why* (investor misperception), the other from *who absorbs and how much* (liquidity-provider balance sheets). In tranquil markets, these forces are separable and belief dispersion dominates. Under stress, however, belief-driven imbalances can trigger inventory pressures, implying that both mechanisms coexist, with their relative importance varying by regime.

7 State-Dependent Amplification of Confusion Shocks

To assess whether confusion shocks are amplified under market stress, we estimate post-event responses in liquidity and order flow as a function of stress conditions. We define post-event window indicators Post_{0-10} and Post_{0-30} for the 10-minute and 30-minute intervals following each event, respectively. Market stress is proxied by a top-decile dummy of the daily VIX, denoted $\text{HighStress}_{10} = \mathbf{1}\{\text{VIX} \geq p90\}$. For each dependent variable $Y_{i,e,t}$, we estimate a pooled difference-in-differences regression of the form:

$$\log Y_{i,e,t} = \theta (\text{Treat}_i \times \text{Post}_w) + \delta (\text{Treat}_i \times \text{HighStress}_{10,e} \times \text{Post}_w) + \gamma' X_{i,e,t} + \alpha_i + \delta_e + \varepsilon_{i,e,t}, \quad (8)$$

where i indexes securities, e event dates, and t minutes within the window w . The coefficient θ captures the low-stress effect of the shock, while δ measures the incremental high-stress response. The net high-stress effect is $\theta + \delta$, with the corresponding economic effect $\exp(\theta + \delta) - 1$.

Control variables $X_{i,e,t}$ include log turnover and log realized volatility. We include fixed effects for both security (α_i) and event date (δ_e). Standard errors are heteroskedasticity-robust (HC1) and, in robustness, two-way clustered at the security and event-time levels. All dependent variables are in logs, so coefficients are directly interpretable as percentage effects.

We analyze five key outcomes – spreads, depth, order imbalance, price impact, and order-flow volatility. Each variable captures a distinct margin of market liquidity. Effective Spread (efspread) is the log difference between transaction price and midquote, where a widening indicates higher trading costs or constrained inventory capacity. Depth is the log sum of bid and ask sizes. We also compute a *baseline-normalized depth* as $\log \text{depth}_t - \overline{\log \text{depth}}_{[-60,-31]}$ to capture relative depth withdrawal around the event. Order Imbalance Magnitude ($|\text{OI}|$) is measured as the absolute net order flow per event bin, capturing directional intensity of trading following confusion shocks. Price Impact is measured as (λ) : $\log |r_t| - \log |\text{OI}_t|$, where higher λ implies greater sensitivity of prices to order flow. We winsorize this variable at 1% tails to mitigate denominator noise. Finally, we have two measures of Order-Flow Volatility: (i) *OI volatility* = $\log \text{sd}(\text{oi}_t)$, the volatility of signed net flow; and (ii) *Arrival volatility* = $\log \text{sd}(\text{buy_count}_t + \text{sell_count}_t)$, capturing clustering of order arrivals. Both measures are computed within 0–10 and 0–30 minute windows. All variables are computed for each (security, event) using 1-minute resolution data. Volatility measures are winsorized at the 1st and 99th percentiles, and we exclude windows with fewer than six valid observations.

Table 11 reports estimated coefficients and economic magnitudes for the post-shock effects under low- and high-stress regimes. In tranquil markets, confusion shocks have mild or short-lived effects: spreads remain nearly unchanged, depth declines modestly, and price impact is stable. Under high stress (top-decile VIX), the same shocks trigger stronger and more persistent adjustments across all liquidity dimensions. For liquidity costs, spreads widen by about 19% under stress, consistent with tighter dealer risk capacity; depth initially falls (24%) but recovers quickly (+12%), indicating transient, not structural, liquidity withdrawal. Order imbalance magnitude rises by roughly 8%, while price impact (λ) surges—by 65% within 30 minutes. This pattern suggests that belief dispersion generates the initial dislocation, while balance-sheet frictions amplify it as stress binds. Under stress, both signed OI volatility and order-arrival volatility increase sharply. Within 0–10 minutes, signed flow volatility rises by 6.8% and arrival volatility by 35.6%; pooling to 0–30 minutes, both remain elevated (20%). Trading thus becomes more erratic and clustered, reinforcing that stress amplifies confusion shocks through inventory and flow-volatility feedbacks.

Overall, these findings point to orthogonal but state-dependent channels. In tranquil markets, confusion shocks primarily reflect transient belief dispersion with minimal liquidity stress. In

volatile markets, the same shocks propagate through inventory constraints and flow volatility, widening spreads and deepening price impact. The coexistence of cognitive and balance-sheet frictions explains why confusion events are largely benign in normal times but strongly amplified under systemic stress.

8 Conclusion

This paper uses instances where investors mistakenly trade similarly named securities to reveal how modern, automated markets process non-fundamental shocks. Exploiting these naturally occurring ticker-confusion events that generate exogenous disturbances in order flow, we document systematic but short-lived price and liquidity distortions. Prices initially overreact to belief-driven demand imbalances and subsequently reverse, while inventory proxies remain stable, indicating that misperception rather than balance-sheet frictions drives these anomalies.

Our results highlight that two orthogonal mechanisms jointly shape short-term inefficiency. The belief-dispersion channel arises from transient heterogeneity in investors' perceptions and dominates in normal conditions. The inventory-risk channel, in contrast, reflects liquidity-supply frictions that become binding only under stress. The coexistence—but not contradiction—of these forces explains why confusion shocks are largely benign in tranquil periods yet amplified when volatility and funding constraints rise.

These findings extend the literature on temporary price pressure and liquidity provision by showing that behavioral and structural frictions interact in a state-dependent manner. Confusion events offer a clean micro-laboratory for observing how cognitive errors propagate through automated trading ecosystems and how algorithmic liquidity providers absorb or offset them. Ultimately, understanding how belief dispersion and inventory risk jointly influence market adjustment is essential for assessing the resilience of modern financial systems in the face of both human and mechanical error.

References

- Andersen, Torben G, Tim Bollerslev, Francis X Diebold, and Heiko Ebens**, “The distribution of realized stock return volatility,” *Journal of Financial Economics*, 2001, *61* (1), 43–76. [10](#)
- Asriyan, Vladimir, William Fuchs, and Brett Green**, “Liquidity sentiments,” *American Economic Review*, 2019, *109* (11), 3813–3848. [2](#), [3](#)
- Atmaz, Adem and Suleyman Basak**, “Belief dispersion in the stock market,” *The Journal of Finance*, 2018, *73* (3), 1225–1279. [2](#), [3](#)
- Balashov, Vadim S and Andrei Nikiforov**, “How much do investors trade because of name/ticker confusion?,” *Journal of Financial Markets*, 2019, *46*, 100499. [2](#), [12](#), [14](#)
- Bogousslavsky, Vincent and Pierre Collin-Dufresne**, “Liquidity, volume, and order imbalance volatility,” *Journal of Finance*, 2023, *78*, 2189–2232. [2](#), [7](#), [17](#)
- Brogaard, Jonathan, Allen Carrion, Thibaut Moyaert, Ryan Riordan, Andriy Shkilko, and Konstantin Sokolov**, “High frequency trading and extreme price movements,” *Journal of Financial Economics*, 2018, *128* (2), 253–265. [4](#), [6](#)
- , **Terrence Hendershott, and Ryan Riordan**, “High-frequency trading and price discovery,” *The Review of Financial Studies*, 2014, *27* (8), 2267–2306. [6](#)
- Brunnermeier, Markus K and Lasse Heje Pedersen**, “Market liquidity and funding liquidity,” *The review of financial studies*, 2009, *22* (6), 2201–2238. [23](#)
- Chakrabarty, Bidisha, Bingguang Li, Vanthuan Nguyen, and Robert A Van Ness**, “Trade classification algorithms for electronic communications network trades,” *Journal of Banking & Finance*, 2007, *31* (12), 3806–3821. [17](#)
- Hendershott, Terrence and Albert J Menkveld**, “Price pressures,” *Journal of Financial Economics*, 2014, *114* (3), 405–423. [2](#), [4](#)
- , **Charles M Jones, and Albert J Menkveld**, “Does algorithmic trading improve liquidity?,” *The Journal of Finance*, 2011, *66* (1), 1–33. [3](#), [10](#)
- Ho, Thomas and Hans R Stoll**, “Optimal dealer pricing under transactions and return uncertainty,” *Journal of Financial Economics*, 1981, *9* (1), 47–73. [2](#)

- Holden, Craig W and Stacey Jacobsen**, “Liquidity measurement problems in fast, competitive markets: Expensive and cheap solutions,” *The Journal of Finance*, 2014, 69 (4), 1747–1785. [7](#), [17](#)
- Kirilenko, Andrei A and Andrew W Lo**, “Moore’s law versus Murphy’s law: Algorithmic trading and its discontents,” *Journal of Economic Perspectives*, 2013, 27 (2), 51–72. [2](#)
- Kirilenko, Andrei, Albert S Kyle, Mehrdad Samadi, and Tugkan Tuzun**, “The flash crash: High-frequency trading in an electronic market,” *The Journal of Finance*, 2017, 72 (3), 967–998. [4](#), [6](#)
- Levenshtein, V. I.**, “Binary Codes Capable of Correcting Deletions, Insertions and Reversals,” *Soviet Physics Doklady*, feb 1966, 10, 707. [7](#)
- Menkveld, Albert J**, “The economics of high-frequency trading: Taking stock,” *Annual Review of Financial Economics*, 2016, 8 (1), 1–24. [2](#)
- O’hara, Maureen**, “High frequency market microstructure,” *Journal of Financial Economics*, 2015, 116 (2), 257–270. [2](#)
- Rashes, Michael S**, “Massively confused investors making conspicuously ignorant choices (mci–mcic),” *The Journal of Finance*, 2001, 56 (5), 1911–1927. [2](#), [13](#)
- Thompson, Samuel B**, “Simple formulas for standard errors that cluster by both firm and time,” *Journal of Financial Economics*, 2011, 99 (1), 1–10. [16](#), [42](#), [43](#)
- von Beschwitz, Bastian, Donald B Keim, and Massimo Massa**, “First to “read” the news: News analytics and algorithmic trading,” *The Review of Asset Pricing Studies*, 2020, 10 (1), 122–178. [3](#), [10](#), [14](#)

9 Figures

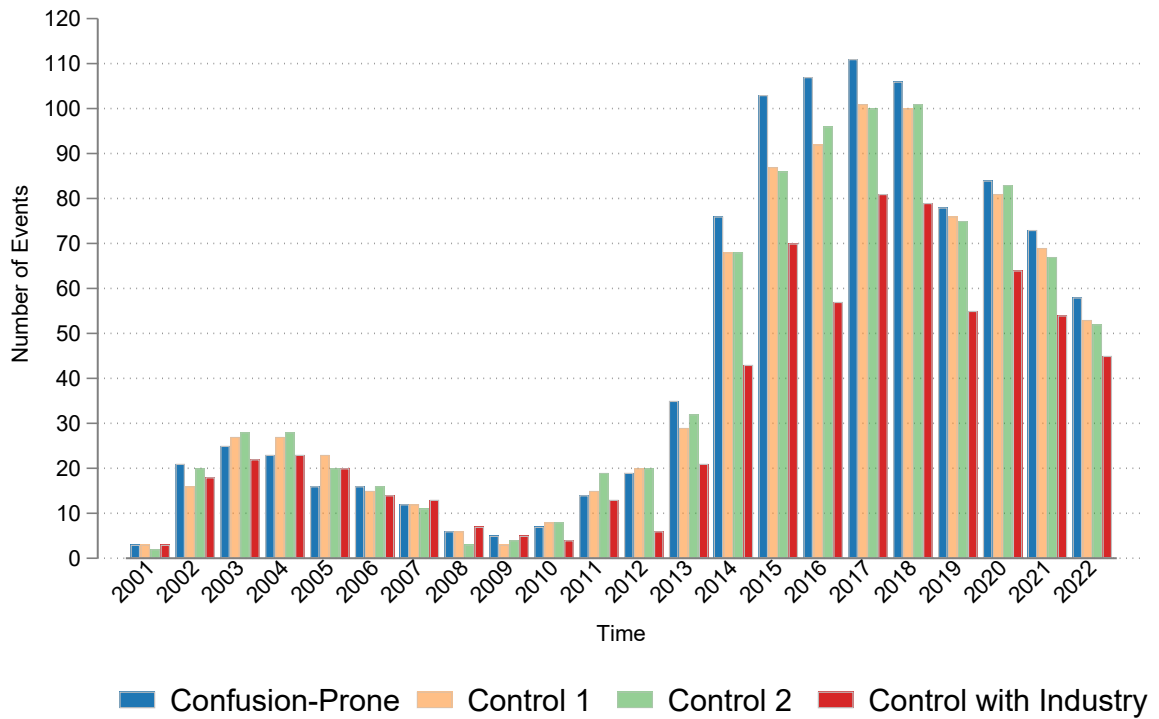


Figure 1: Events over Time

Notes: The figure plots the number of events in the analysis over the period from 2001 to 2022.

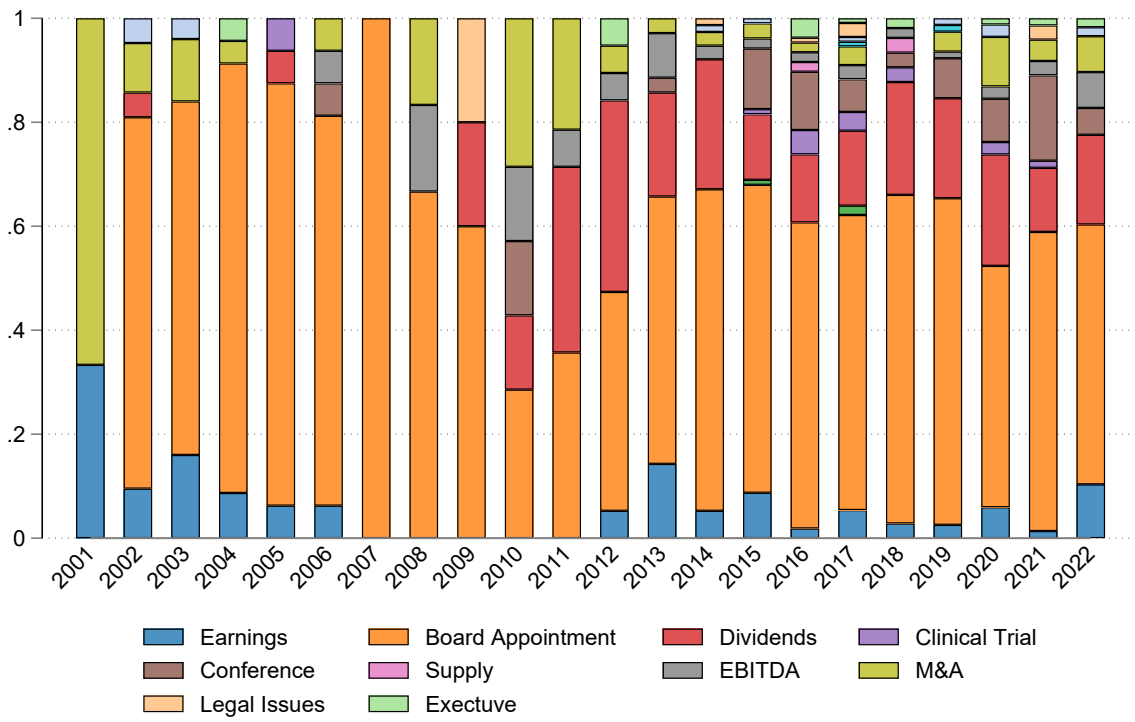


Figure 2: Events over Time

Notes: The figure plots the share of different types of events over the period from 2001 to 2022.

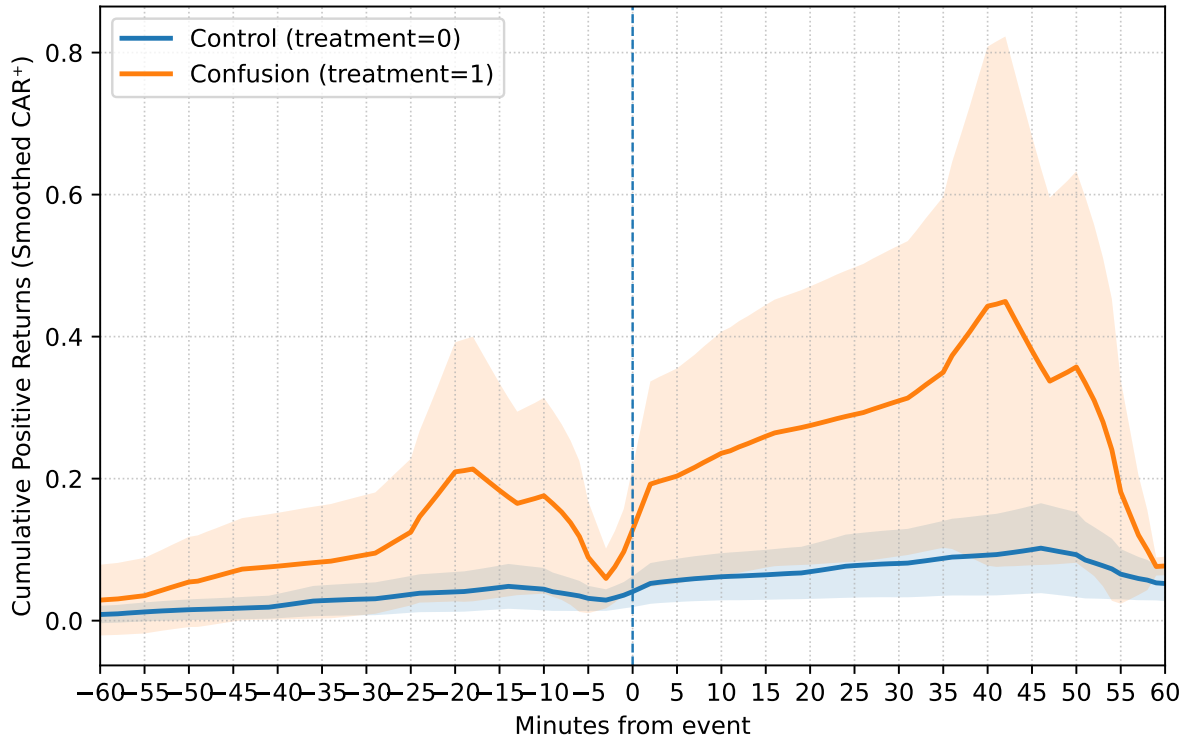


Figure 3: Absolute Cumulative Abnormal Returns

Notes: The figure presents smoothed cumulative positive returns for the *confusion* sample (treatment = 1) and the *control* sample (treatment = 0) over a symmetric event window of ± 60 minutes. The series are smoothed using a centered rolling mean with a 5-minute window to attenuate high-frequency noise and highlight persistent differences in post-event dynamics. Shaded regions correspond to smoothed 95% confidence intervals. The confusion series shows a noticeably stronger upward trajectory after the event, suggesting that ticker confusion events induce more pronounced cumulative positive price movements.

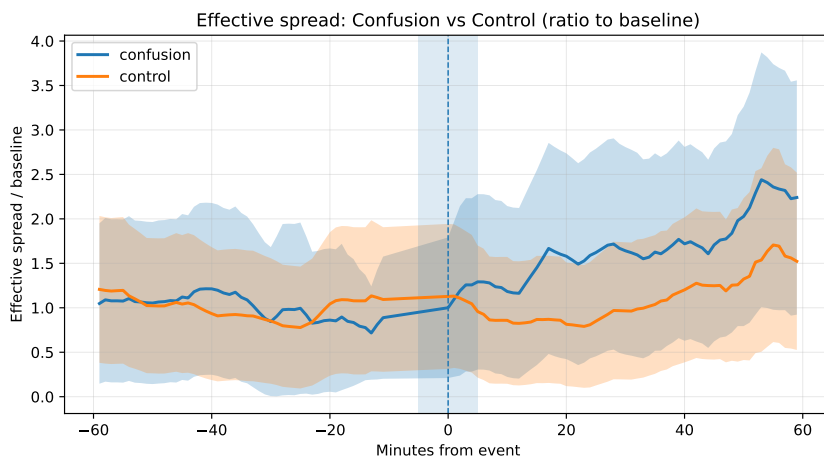


Figure 4: Effective spread for confusion vs. control events.

Notes: This figure plots the effective spread around events for confusion vs control ticker pairs. Shaded areas represent 95 percent confidence intervals. The results show that confusion-prone stocks experience temporary increases in effective spreads, consistent with short-lived liquidity deterioration.

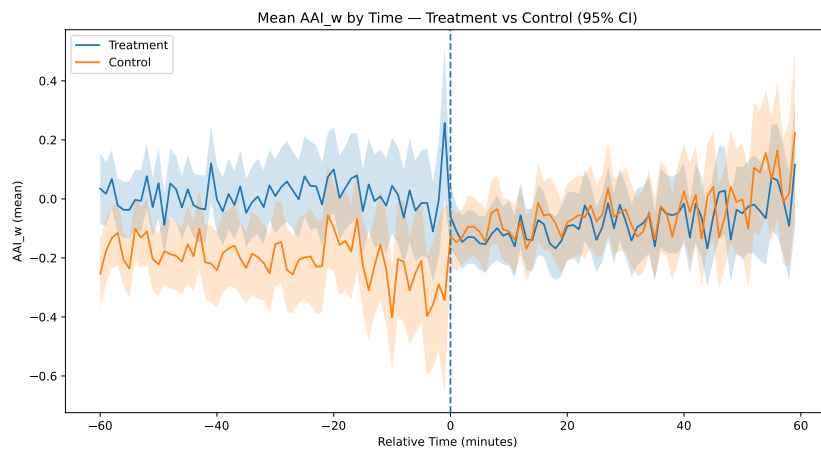


Figure 5: Algorithmic activity for confusion vs. control events.

Notes: The figure plots the mean Algorithmic Activity Index (AAI_w) over a ± 60 -minute window for confusion (treatment) and matched control events. The sharp increase in AAI_w within five minutes before the event indicates a surge in algorithmic order submissions and cancellations. Liquidity conditions remain normal before the shock, implying that confusion events emerge endogenously through algorithmic execution rather than in anticipation of news or stress.

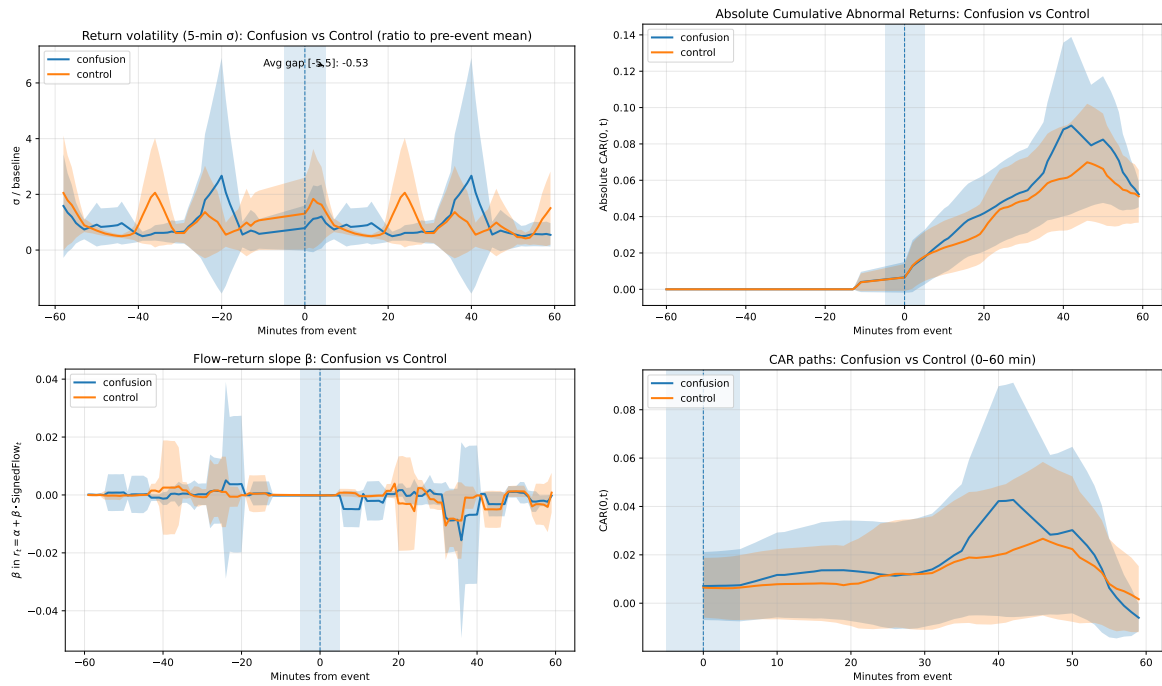


Figure 6: Confusion versus Control Stocks Around Events.

Notes: The figure compares event-time dynamics for confusion-prone and control stocks over the $[-60, +60]$ -minute window. Panel (A) shows a spike in short-term return volatility; Panel (B) plots absolute cumulative abnormal returns, highlighting transient price swings; Panel (C) reports weakened order-flow–return sensitivity during confusion; and Panel (D) shows rapid post-event reversal within an hour. Shaded areas represent 95 percent confidence intervals. Together, the evidence supports the misperception mechanism over inventory frictions.

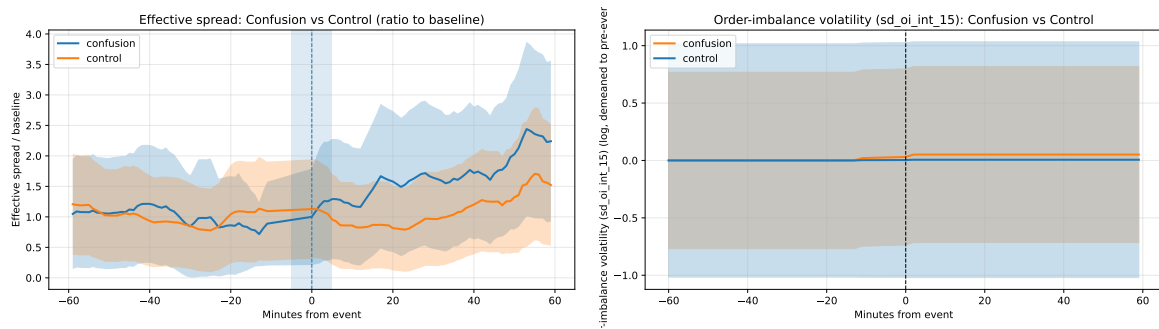


Figure 7: Liquidity costs and order-flow volatility during confusion vs. control events.

Notes: Figures plot effective spread and order-flow volatility around confusion vs control events. Shaded areas represent 95 percent confidence intervals. The results show that confusion-prone stocks experience temporary increases in effective spreads (left), consistent with short-lived liquidity deterioration, and plot the standard deviation of order imbalance over 15-minute intervals (right), indicating that confusion episodes do not trigger inventory stress but reflect transitory trading noise.

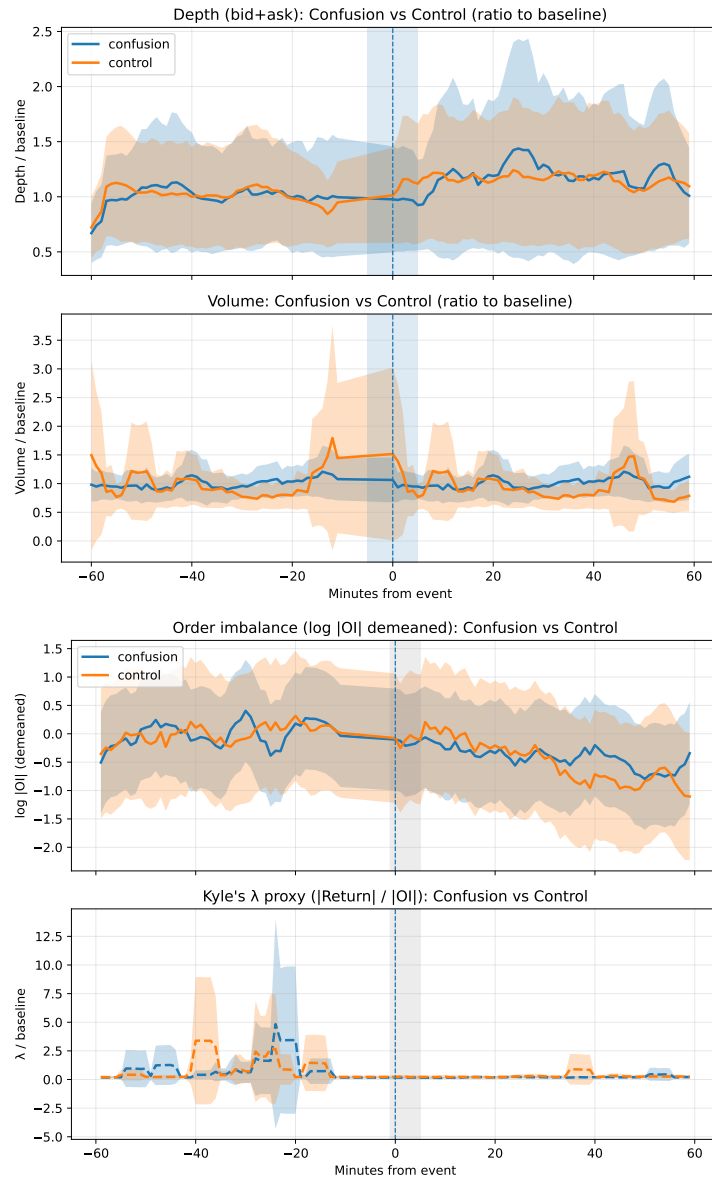


Figure 8: Liquidity responses during confusion vs. control events.

Notes: From top to bottom, Figures show changes in depth and volume; order imbalance and price-impact proxy (Kyle's λ). Shaded areas represent 95 percent confidence intervals. Figures show that confusion episodes temporarily disrupt liquidity but recover within 30–60 minutes.

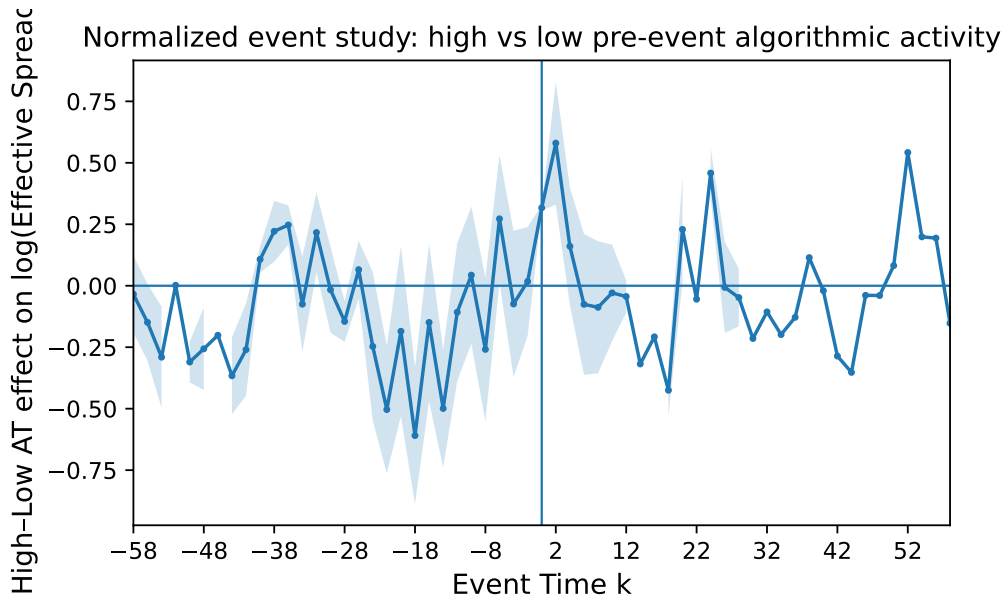


Figure 9: Stacked DiD: Effective spread response by algorithmic intensity.

Notes: High-AT stocks exhibit transitory spread increases that revert quickly, whereas low-AT stocks display persistent widening, indicating slower recovery when algorithmic participation is low.

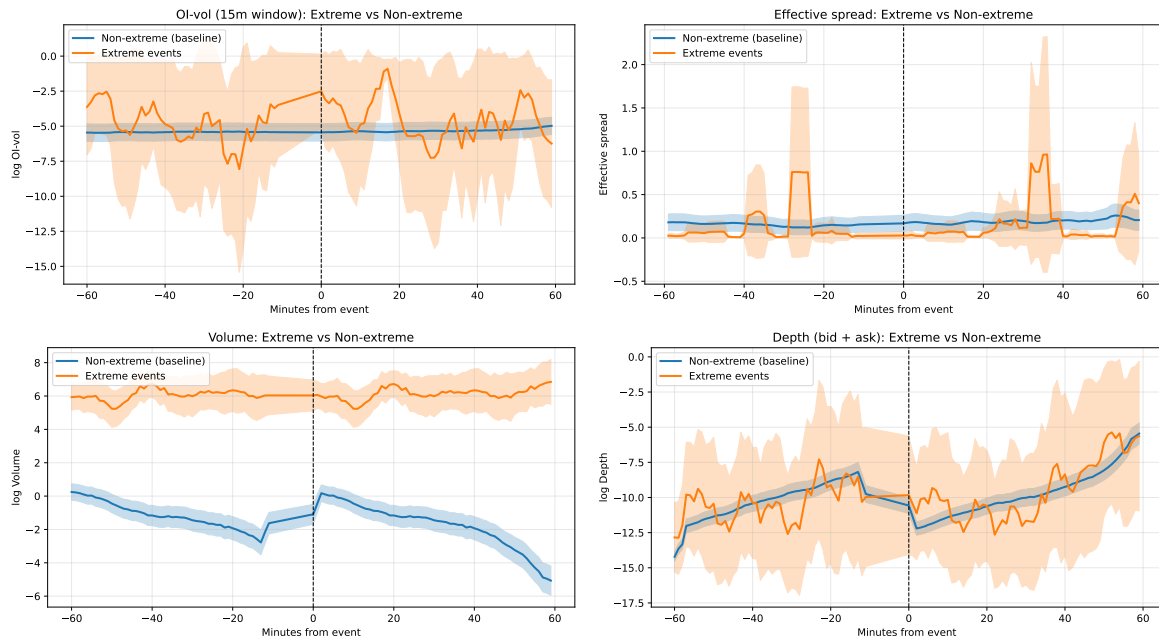


Figure 10: **Market dynamics under confusion and extreme events.** This figure compares the average event-time behavior of (i) order imbalance volatility, (ii) effective spread, (iii) trading volume, and (iv) market depth around confusion-prone and extreme events. Extreme events are defined as the top 1 percent of absolute intraday returns within each stock. Order imbalance volatility and market depth are computed over rolling 15-minute intervals. Shaded areas represent 95 percent confidence intervals. The results show that order imbalance volatility, spreads, and volume rise sharply while market depth collapses during extreme events—consistent with binding inventory and liquidity constraints. In contrast, none of these variables move significantly during confusion events, suggesting that ticker-confusion mispricing originates from belief dispersion rather than liquidity stress.

10 Tables

Table 1: Descriptive Statistics

	(1) All	(2) Confusion-prone	(3) Control group	(4) T-test
Effective Spread. %	0.21 (1.12)	0.19 (1.11)	0.24 (1.15)	-0.056 [-0.610]
CAR	-0.039 (0.75)	-0.042 (0.85)	-0.036 (0.58)	-0.0061 [-0.168]
Turnover	0.11 (0.61)	0.098 (0.55)	0.12 (0.69)	-0.021 [-0.701]
Volatility	0.00021 (0.00049)	0.00023 (0.00051)	0.00017 (0.00047)	0.000063*** [2.627]
ALGO Trading	-153.7 (1387.5)	-114.3 (1071.2)	-217.6 (1786.2)	103.3 [0.899]
ALGO Trading, before	-3.67 (18.0)	-2.91 (6.35)	-4.71 (26.6)	1.80** [2.056]
ALGO before, high	-0.57 (0.35)	-0.59 (0.34)	-0.55 (0.36)	-0.038 [-1.603]
Market Capitalization	1447743.8 (2411956.0)	1384533.5 (2314437.2)	1534159.9 (2538290.8)	-149626.4 [-1.274]
Composite Sentiment Score	0.043 (0.050)	0.043 (0.049)	0.043 (0.051)	0.00067 [0.275]
Observations	1728	998	730	1728

Notes: This table reports the descriptive statistics for individual asset characteristics. The first column describes all assets, i.e. both Confusion-prone tickers and the control group. Column 2 describes Confusion-prone tickers and Column 3 describes the control group with industry match. The differences in means between Confusion-prone tickers and the control groups are presented in Column (4), where t-statistics are reported in brackets. In the table effective spread is the effective spread (in basis point), volatility is the realized volatility computed using midpoint returns, CAR is the cumulative abnormal returns over 60 minutes after the event, Composite Sentiment Score ranges from -1 (extremely negative) to +1 (extremely positive) and a story-level sentiment that combines various sentiment measures, such as the price reaction to the news. Standard deviations are in parentheses. *, **, and *** denote significance at the 10%, 5% and 1% levels, respectively.

Table 2: Distributions of CARs

	mean	sd	p1	p5	p10	p25	p50	p75	p90	p95	p99
Control, Industry	-0.00	0.02	-0.06	-0.03	-0.02	-0.01	-0.00	0.01	0.02	0.03	0.08
Confusion-prone	-0.04	0.85	-2.77	-0.20	-0.03	-0.01	-0.00	0.01	0.02	0.07	0.77
All	-0.02	0.65	-1.54	-0.05	-0.02	-0.01	-0.00	0.01	0.02	0.04	0.41

Notes: This table reports and compares the means and selected deciles of the CAR distributions for the control and confusion-prone groups of stocks

Table 3: CARs and sentiment alignment

	Confusion-prone			Control group		
	(1) CAR	(2) CAR	(3) CAR	(4) CAR	(5) CAR	(6) CAR
Composite Sentiment Score	1.186** (0.578)	1.203** (0.589)	1.202** (0.591)	-0.140 (0.495)	-0.129 (0.509)	-0.127 (0.511)
log Market Capitalization		0.002 (0.037)	-0.000 (0.039)		-0.010 (0.031)	-0.007 (0.032)
log Turnover		0.032* (0.019)	0.032* (0.019)		0.001 (0.014)	0.001 (0.014)
ALGO, above median			-0.017 (0.075)			0.034 (0.060)
Observations	995	970	969	727	705	704

Notes: This table reports the regression results with CAR as the dependent variable and log market capitalization, composite sentiment index, and algorithmic activity before the event. The first three columns provides the results for confusion-prone stocks, and the last three columns provides the results for a control group consisting of stocks matched on size and industry. Standard deviations are in parentheses. *, **, and *** denote significance at the 10%, 5% and 1% levels, respectively.

Table 4: Return Correlation: Treatment vs Control Groups

	(1) Treatment	(2) Control
$Return_{i,t}^{tick1}$	$1.23 \times 10^{-5***}$ (1.46×10^{-6})	-1.805×10^{-8} (1.152×10^{-6})
$Return_{i,t-1}^{tick1}$	2.798×10^{-7} (1.47×10^{-6})	-1.12×10^{-7} (1.157×10^{-6})
$Return_{i,t-1}^{tick2}$	$-0.137***$ (0.0038)	$-0.0118***$ (0.0022)
Constant	$0.002***$ (0.0006)	$0.0016***$ (0.0005)
Observations	82,792	218,288
FE	Yes	Yes

Notes: Entity fixed effects included. Robust standard errors in parentheses. *** $p < 0.01$, ** $p < 0.05$, * $p < 0.1$. Significant correlation observed only in the treatment group.

Table 5: Stacked Event–Time DiD: Effective Spread

	(1)	(2)	(3)	(4)
	Baseline	+ Depth Controls	+ Intraday Shape	High-Confusion Events
Panel A. Treatment \times Event-Time Bins (ref: $[-30, -11]$; exclude $[-10, -1]$)				
[0, 10]	0.115***	0.111***	0.108***	0.320***
	(0.043)	(0.021)	(0.022)	(0.058)
[11, 30]	0.063**	0.049**	0.046**	0.140**
	(0.022)	(0.020)	(0.021)	(0.057)
[31, 60]	0.000	0.015	0.013	0.041
	(0.017)	(0.016)	(0.016)	(0.048)
$[-60, -31]$	0.000	0.003	0.003	0.004
	(0.004)	(0.004)	(0.005)	(0.009)
<i>Controls and Fixed Effects</i>				
log(Turnover)	Yes	Yes	Yes	Yes
log(RetVol)	Yes	Yes	Yes	Yes
Bid/Ask Depth	No	Yes	Yes	Yes
Ticker FE (α_i)	Yes	Yes	Yes	Yes
Event FE (ψ_e)	Yes	Yes	Yes	Yes
Intraday shape (common k FEs)	No	No	Yes	Yes
<i>Joint Tests (p-values)</i>				
Pre-trend: $[-60, -31]$	1.00	0.69	0.66	0.81
Post: [0, 10]	0.00	0.00	0.00	0.00
Durability: [11, 30]	0.01	0.02	0.03	0.01
Late: [31, 60]	0.28	0.31	0.35	0.39
Within- R^2	0.0023	0.0025	0.0026	0.0024
Observations	37,500	37,500	37,500	12,600

Notes: Dependent variable is $\log(\text{Effective Spread})$. Coefficients are interactions of ConfusionProne_i with event-time bins; reference bin is $[-30, -11]$. The last 10 pre-event minutes $[-10, -1]$ are excluded to mitigate potential leakage. Columns (1)–(3) use the full sample; Column (4) restricts to “high-confusion” events (e.g., significant CARs). Ticker and event fixed effects included throughout. Standard errors are double-clustered by relative minute and ticker–event pair following [Thompson \(2011\)](#). ***, **, * denote significance at the 1%, 5%, 10% levels. Panel B converts log-point coefficients to percentage and basis-point effects: $\% \Delta = 100 \times (e^{\hat{\beta}} - 1)$ and $\text{bps} = 37.16 \times (e^{\hat{\beta}} - 1)$ at the sample median spread. For instance, $[0, 10] = 0.115$ implies $+12.15\%$ or $+4.52$ bps. High-confusion events correspond to cases with significant CARs; coefficients in Column (4) are approximately three times larger. Wild-cluster bootstrap p -values for $[0, 10]$ remain < 0.01 across all specifications.

Table 6: Stacked Event-Time DiD: Volatility of Order Imbalance

	(1)	(2)	(3)	(4)
	Baseline	+ Depth Controls	+ Intraday Shape	High-Confusion Events
<i>Treatment × Event-Time Bins (ref: $[-30, -11]$; exclude $[-10, -1]$)</i>				
[0, 10]	0.009 (0.018)	0.007 (0.019)	0.008 (0.020)	0.015 (0.022)
[11, 30]	0.003 (0.017)	0.002 (0.017)	0.004 (0.018)	0.009 (0.021)
[31, 60]	0.001 (0.015)	0.000 (0.016)	0.001 (0.016)	0.003 (0.019)
$[-60, -31]$	0.002 (0.014)	0.001 (0.014)	0.001 (0.015)	0.003 (0.018)
<i>Controls and Fixed Effects</i>				
log(Turnover)	Yes	Yes	Yes	Yes
log(RetVol)	Yes	Yes	Yes	Yes
Bid/Ask Depth	No	Yes	Yes	Yes
Ticker FE (α_i)	Yes	Yes	Yes	Yes
Event FE (ψ_e)	Yes	Yes	Yes	Yes
Intraday shape (common k FEs)	No	No	Yes	Yes
<i>Joint Tests (p-values)</i>				
Pre-trend: $[-60, -31]$	0.74	0.70	0.68	0.77
Post: [0, 10]	0.63	0.65	0.60	0.58
Durability: [11, 30]	0.79	0.82	0.80	0.75
Late: [31, 60]	0.88	0.85	0.83	0.81
Observations	N	N	N	N (High-conf)
R^2	0.69	0.70	0.70	0.69

Notes: Dependent variable is $\log(\text{VolOI})$, where VolOI is the standard deviation of signed order imbalance over a 5-minute rolling window. Coefficients are interactions of ConfusionProne_i with event-time bins; reference bin is $[-30, -11]$. The last 10 pre-event minutes $[-10, -1]$ are excluded to mitigate potential information leakage. Columns (1)–(3) use the full sample; Column (4) restricts to “high-confusion” events (e.g., significant CARs). Ticker and event fixed effects are included throughout. Standard errors are double-clustered by relative minute and ticker-pair-event following [Thompson \(2011\)](#).

All coefficients are economically small and statistically indistinguishable from zero, implying that order-imbalance volatility remains stable throughout confusion episodes.

Table 7: Stacked Event–Time DiD: Trading Volume (log)

	(1)	(2)	(3)	(4)
	Baseline	+ Depth Controls	+ Intraday Shape	High-Confusion Events
<i>Treatment × Event-Time Bins (ref: [−30, −11]; exclude [−10, −1])</i>				
[0, 10]	-0.139***	-0.138***	-0.139***	-0.181***
	(0.038)	(0.035)	(0.036)	(0.057)
[11, 30]	-0.126**	-0.120**	-0.123**	-0.162**
	(0.051)	(0.049)	(0.050)	(0.064)
[31, 60]	-0.039	-0.031	-0.028	-0.045
	(0.044)	(0.043)	(0.043)	(0.055)
[−60, −31]	0.002	0.004	0.003	0.006
	(0.006)	(0.006)	(0.007)	(0.008)
<i>Controls and Fixed Effects</i>				
log(Turnover)	Yes	Yes	Yes	Yes
log(RetVol)	Yes	Yes	Yes	Yes
Bid/Ask Depth	No	Yes	Yes	Yes
Ticker FE (α_i)	Yes	Yes	Yes	Yes
Event FE (ψ_e)	Yes	Yes	Yes	Yes
Intraday shape (common k FEs)	No	No	Yes	Yes
<i>Joint Tests (p-values)</i>				
Pre-trend: [−60, −31]	0.64	0.61	0.59	0.68
Post: [0, 10]	0.00	0.00	0.00	0.00
Durability: [11, 30]	0.02	0.02	0.03	0.01
Late: [31, 60]	0.31	0.33	0.35	0.37
Within- R^2	0.0021	0.0022	0.0022	0.0023
Observations			37,500	

Notes: Dependent variable is $\log(1 + \text{Volume})$. Coefficients are interactions of ConfusionProne_i with event-time bins; reference bin is $[-30, -11]$. The pre-window $[-10, -1]$ is excluded. Standard errors are double-clustered by relative minute and event–ticker pair. ***, **, * denote significance at the 1%, 5%, 10% levels.

Table 8: Stacked Event-Time DiD: Quoted Depth

	(1)	(2)	(3)	(4)
	Baseline	+ Depth Controls	+ Intraday Shape	High-Confusion Events
<i>Treatment \times Event-Time Bins (ref: $[-30, -11]$; exclude $[-10, -1]$)</i>				
[0, 10]	-0.061 *** (0.020)	-0.060*** (0.019)	-0.059*** (0.019)	-0.089*** (0.028)
[11, 30]	-0.035* (0.018)	-0.032* (0.017)	-0.031* (0.017)	-0.046** (0.021)
[31, 60]	0.018 (0.019)	0.022 (0.018)	0.021 (0.018)	0.028 (0.022)
$[-60, -31]$	0.002 (0.005)	0.003 (0.005)	0.002 (0.005)	0.004 (0.007)
<i>Controls and Fixed Effects</i>				
log(Turnover)	Yes	Yes	Yes	Yes
log(RetVol)	Yes	Yes	Yes	Yes
Bid/Ask Depth	No	Yes	Yes	Yes
Ticker FE (α_i)	Yes	Yes	Yes	Yes
Event FE (ψ_e)	Yes	Yes	Yes	Yes
Intraday shape (common k FEs)	No	No	Yes	Yes
<i>Joint Tests (p-values)</i>				
Pre-trend: $[-60, -31]$	0.71	0.68	0.66	0.70
Post: [0, 10]	0.00	0.00	0.00	0.00
Durability: [11, 30]	0.03	0.03	0.04	0.02
Late: [31, 60]	0.24	0.27	0.28	0.29
Within- R^2	0.0030	0.0031	0.0032	0.0031
Observations			37,500	

Notes: Dependent variable is $\log(1 + \text{Depth}_{\text{bid}} + \text{Depth}_{\text{ask}})$. Coefficients compare confusion-prone to matched controls by event-time bin. Standard errors are double-clustered by relative minute and event-ticker pair. ***, **, * denote significance at the 1%, 5%, 10% levels.

Table 9: Speed of Adjustment of CARs

	CAR Adjustment			Negative CAR Adjustment		
	(1) All	(2) Confusion	(3) Control	(4) All	(5) Confusion	(6) Control
Confusion Event	16.76905*** (3.51760)			-5.74083 (5.65833)		
Algorithmic Trading, Rescaled	0.00966 (0.02098)	-0.15857*** (0.02878)	0.01079 (0.02036)	0.04344 (0.03307)	0.10170** (0.04580)	0.04302 (0.03340)
Confusion Event \times Algorithmic Trading, Rescaled	-0.16774*** (0.03518)			0.05752 (0.05659)		
Constant	-1.05472 (2.09733)	15.76477*** (2.87765)	-1.17021 (2.03604)	-3.78029 (3.30697)	-9.60122** (4.58014)	-3.73199 (3.33979)
Observations	15673	9512	6161	15673	9512	6161

Notes: This table reports the speed of adjustment of CARs and its determinants for Treated and Control groups. In columns (1)-(3) regression results for the equation (??). Standard deviations are in parentheses. *, **, and *** denote significance at the 10%, 5% and 1% levels, respectively.

Table 10: High–Low Algorithmic Activity Difference

Window	$\bar{\beta}_{\text{norm}}$	SE	$\Delta\%$	Approx. SE(%)	Δ bps
[0, 5]	0.353**	(0.145)	+42.3	(14.5)	+15.7
[6, 20]	-0.120	(0.119)	-11.3	(11.9)	-4.2

Notes: High–Low AT difference in normalized DiD coefficients, averaged within each event-time window and normalized by pre-event mean $([-10, -2])$. $\Delta\% = 100 \times (e^{\bar{\beta}} - 1)$; Δ bps translates percentage change at the sample-median effective spread (37 bps). Standard errors are clustered by (event \times pair) and relative minute.

High-AT markets experience faster and smaller spread reactions, consistent with algorithmic liquidity provision absorbing confusion-induced noise trading.

Table 11: State-Dependent Amplification of Confusion Shocks

Variable	Window	θ	δ	$\theta + \delta$	Economic Effect
Effective spread	0–10 min	−0.112	+0.070	−0.042	−4.1%
Effective spread	0–30 min	−0.144	+0.316	+0.172	+19.0%
Depth	0–10 min	−0.244	+0.358	+0.113	+12.0%
Depth	0–30 min	−0.234	+0.061	−0.173	−15.9%
Order imbalance OI	0–10 min	+0.055	+0.020	+0.075	+7.8%
Order imbalance OI	0–30 min	+0.029	+0.046	+0.074	+7.7%
Price impact λ	0–10 min	−0.132	+0.157	+0.025	+2.6%
Price impact λ	0–30 min	+0.005	+0.493	+0.498	+64.6%
<i>OI volatility (sd(oi))</i>	0–10 min	+0.026	+0.039	+0.065	+6.8%
<i>Arrival volatility (sd(buys+sales))</i>	0–10 min	+0.079	+0.226	+0.304	+35.6%
<i>OI volatility (sd(oi))</i>	0–30 min	+0.057	+0.120	+0.177	+19.3%
<i>Arrival volatility (sd(buys+sales))</i>	0–30 min	+0.057	+0.146	+0.203	+22.5%

Notes: This table reports estimated post-event effects of confusion shocks on liquidity and order-flow variables across tranquil and high-stress regimes. Event-time regressions are estimated over 0–10 minute (depth, |OI|, λ , volatility, spreads) and 0–30 minute (spreads, depth, |OI|, λ , volatility) windows. θ measures the low-stress effect (Treat \times Post), δ the incremental high-stress effect (Treat \times HighStress₁₀ \times Post), and $\theta + \delta$ the total effect under high stress. Economic effects are expressed as $\exp(\theta + \delta) - 1$. All specifications include log turnover and log volatility as controls, as well as security and event-date fixed effects. Robust HC1 standard errors are reported; results are robust to two-way clustering (security \times event-time).